For presentation at the AIAA / ASME Wind Energy Symposium, Reno Nevada Jan 6-9 1997

CONF-970135--14

SAND96-2520C
SAND--96-2520C

ACOUSTIC EMISSION MONITORING OF A WIND TURBINE BLADE DURING A FATIGUE TEST

A.G. Beattie
Department 9742
Sandia National Laboratories
Albuquerque NM, 87185-0615

This work was supported by the United States Department of Energy under Contract DE-AC04-94AL85000.
Sandia is a multiprogram laboratory operated by Sandia Corporation, a Lockheed Martin Company, for the United States Department of Energy.

Abstract

A fatigue test of a wind turbine blade was conducted at the National Renewable Energy Laboratory in the fall of 1994. Acoustic emission monitoring of the test was performed, starting with the second loading level. The acoustic emission data indicated that this load exceeded the strength of the blade. From the first cycle at the new load, an oil can type of deformation occurred in two areas of the upper skin of the blade. One of these was near the blade root and the other was about the middle of the tested portion of the blade. The emission monitoring indicated that no damage was taking place in the area near the root, but in the deforming area near the middle of the blade, damage occurred from the first cycles at the higher load. The test was stopped after approximately one day and the blade was declared destroyed, although no gross damage had occurred. Several weeks later the test was resumed, to be continued until gross damage occurred. The upper skin tore approximately one half hour after the cycling was restarted.

Test Description

The wind turbine blade tested was a modified base line prototype of a twenty meter blade. It was mounted horizontally in a flap direction with its root attached to a rigid steel mounting assembly. The outer 35% of the blade was removed to prevent it from hitting the roof of the building. The stub was covered and a hydraulic actuator was attached at the stub end. This actuator was capable of exerting a vertical force of about 28,000 lbs., with a maximum displacement of twenty inches. The actuator was operated sinusoidally at 0.75 Hz giving a maximum of 64,800 cycles per day. All tests were run with a positive load only, extending from 10% of peak load to peak load and back to 10%.

The acoustic emission was detected with a Physical Acoustics Corporation (PAC) Spartan AT acoustic emission system. This system has 24 data channels. Every channel can measure and record several parameters for each acoustic emission signal. Parameters collected in this test were the acoustic emission count, the signal length, the signal rise time, the signal peak amplitude (in dB above 1 microvolt out of the sensor) and the area under the signal voltage-time curve (signal strength). The system measures and records the absolute time of signal arrival at the sensor to within about 0.25 microseconds and assigns the approximate load at the time of the signal. This load is sampled 100 times per second but assigned to the hit only after the data arrives at the main computer. Data pile up can cause the load to be as much as thirty seconds out of synchronization with the actual signal arrival time. Therefore the "measured" load can be a misleading parameter in this type of test. This system had the capacity to collect a one gigabyte data file on the hard disk before the data had to be transferred to storage. Such a file would hold

DISCLAIMER

parameters from over 40 million emission signals.

PAC R6I sensors were used in this test. These sensors have an integral 40 dB preamplifier built into them which is powered from the main system through the signal cable. The peak sensitivity of the sensors is near 60 KHz with reasonable response to below 30 KHz. The sensors were applied to the blade with GE Silicone II household cement and sealer, used as both glue and acoustic couplant. Previous tests have shown that this is both a good couplant and an excellent glue for fatigue tests.

The first segment of this test consisted of one million cycles at a peak load of 7,860 lbs. Failure was not anticipated at this load so there was no acoustic monitoring of this segment. The load was then increased by 25 % to 9535 lbs. The root region adjacent to the mounting flange was not thought to be a problem because of extra fiberglass reinforcement around the first four feet of the blade. One sensor was placed on this reinforcement next to the flange to detect any acoustic signals propagating into the blade from the steel mounting assembly, a problem that had been encountered in a previous test.

A brief run at the new load showed that oil canning of the upper blade skin was taking place in two areas. The acoustic emission sensor array was then designed to cover these two areas as well as the root region just outside of the reinforced region. The complete sensor layout is shown in Figure 1. Sensor 24 was placed 60 inches past the top surface array to detect any acoustic signals traveling down the blade from the actuator.

The root array consisted of two rows of four sensors each, one row offset by 45 degrees from the other, covering the region with eight adjacent triangles. The sensor spacing in a row was 41 inches and the rows were 40 inches apart. Because of the high attenuation of fiberglass, this was as far apart as the sensors could be placed with some assurance that moderate amplitude emission sources would be detected at all three sensors of a triangle. Ideally, more sensors would have been used on this region but, with only 24 channels available, that would have precluded two-dimensional location in the oil can regions.

The sensor array on the surface of the blade consisted of two rows of seven sensors each, set up to form a pattern of adjoining rectangles. The row near the front of the blade was set approximately on top of the front spar and the second row was set roughly on top of what appeared to be a second spar. Spacing between the sensors in each row was 30 inches with about 30 inches between rows (the two spars were not parallel). The advantage of this array is that by requiring all four sensors in a rectangle to be hit, one has a better screen to remove "accidental events" (apparent events where non-related signals arrive at the sensors in a correct time sequence).

A previous fatigue test of a wind turbine blade had shown that many acoustic signals were detected during a single fatigue cycle. The largest number occurred during the times of the maximum rate of the load change, both on increasing and decreasing loads. These events were thought to be caused, at least in part, by rubbing of non-bonded surfaces in the blade. In any case, they did not arise from fatigue damage in the previous test. For this blade, initial measurements showed a data rate of about 40 megabytes per hour. To reduce the amount of data collected and to keep primarily signals that were produced by fatigue damage, a voltage controlled gate was used with the system. The gate was triggered off the load cell and permitted the system to take data only when the load was above 8500 lbs. This procedure reduced the collected data rate to about 10 megabytes per hour. While this is still far too high, it did allow the collection of four days' worth of data at this rate before the disk was full. Figure 2 shows the assigned load of all the hits collected on one cycle for assigned loads above 8500 lbs. The loads are plotted as a function of test time. The two located events on this cycle are given as circled crosses. The approximate load curve is shown as a solid line. It is apparent that the assigned loads were close to the actual loads, but both the quantization errors and some scatter are present. Both located events occur very close to the peak load as was expected. This curve suggests that no significant data would be lost by raising the minimum load for event acceptance to a value of 9000 lbs. This was done for the later test stages.

Summary of Test Procedure

The test proceeded in four stages. In the first stage, three and a half minutes of data was taken to determine the initial data rate. Well over an hour of running time was then used in getting the voltage-controlled gate set and working. The second stage was to be the start of the main run. This proceeded for an hour and eighteen minutes, at which time it was stopped because of problems with the loading equipment. The third stage was started the next morning and was continued for 23 hours. It was stopped because the blade surface in one of the oil can regions appeared to be disintegrating and loud noises were occurring on every cycle. The blade was declared failed. The manufacturer then wanted the blade taken to obvious failure, so the fourth stage was started several weeks later. This test lasted for a total of 36 minutes of running time with several stops to examine the blade. The upper skin in the suspect oil can region buckled and pulled away from the front spar. The loading was stopped and a tear in the skin along the edge of the spar was examined. Loading was restarted and continued for another six minutes when the skin buckled and tore perpendicular to the spar with apparent damage to the spar. This ended the test.

Data Analysis

In the analysis of this data, several terms describing the acoustic emission will be used. An event is the localized damage occurring in the blade which produces the acoustic pulse or burst. A hit is defined when the acoustic burst arrives at a sensor and is detected by that sensor. Thus one event will usually produce hits on several sensors. A located event in this paper is when an event produces hits at sensors located at three corners of a triangle for sensors 2 through 9 or at four corners of a rectangle for sensors 10 through 23. The four sensors have to be hit within a time span of 350 microseconds and their arrival times must yield a calculated location within the rectangle formed by the "hit" sensors. An acoustic velocity of 0.14 inches/microsecond was used for analysis.

The initial Spartan AT program used in this test had an unknown bug in its graphing routine. This prevented the accurate presentation of the location data in real time for the first three stages of the test. The error had no effect on the data collection but prevented the experimenters from realizing that damage was occurring in the oil can region located in the rectangle formed by sensors 18, 19, 21 and 20. Analysis of stage one and stage two data at Sandia immediately showed up the problem and a corrected version of the program was sent by the manufacturer. This new version was used in the last stage.

Final analysis of the data was performed by a location program, written in Fortran at Sandia. This program used a non-linear least squares routine to calculate the location from an over determined data set which included arrival times from all four corner sensors of the rectangle. While locations could be calculated from the first three sensors hit, this approach produced a very large number of locations. Because of the high data rate, it was felt that a source which excited all four sensors in a rectangle during an appropriate time window had a high probability of being real instead of an accidental arrival of random signals at the sensors. Two more criteria were applied to the calculated locations. Since the data was an over determined set, any errors in the time measurements would result in a less than perfect fit of the calculated location to the data. The non-linear least squares fitting program calculates a parameter which is an indication of the goodness of the fit. Any data set which did not produce a reasonable value of this parameter was discarded. The rejection criteria was arrived at after extensive experimentation with the program on a variety of data sets. The other criteria was that any location more than 4 inches outside of the edges of the rectangle from which it was calculated (in the length direction of the blade only) was discarded. There were more than sufficient data points remaining to show just where the damage was located. At most, discarding these points would give a slight underestimate of the intensity of the damage.

With the magnitude of the damage that was occurring in this blade, a small fraction of the total number of emissions is more than capable of defining the damaged regions.

Examination of the raw data showed many sets from individual sensors which had signal rise times of only a few microseconds (for this system, the signal rise time is defined as the time between the first detection of the signal and the time of occurrence of the peak amplitude). The frequency dependent attenuation of fiberglass is such that only very large events will have frequency components above 100 KHz. Typical acoustic emission signals which have propagated from growing flaws will take several cycles of their dominant frequency to reach their peak amplitude. One cycle of a 50 KHz wave lasts 20 microseconds. Therefore, all signals with rise times less than 20 microseconds were declared invalid. This does not mean that the signals were not real acoustic emission signals. What usually happens is that the system rearms in the middle of a signal and immediately triggers so that the signal actually started before the start time assigned it by the system. Thus such a signal, while able to point to the occurrence of damage, is useless in determining the location of the signal source. To remove erroneous locations all hits with rise times less than 20 microseconds were filtered from the data sets before the sets were analyzed for the source locations.

Test Results, Stage 1

The acoustic emission system was set up and run for about 3.4 minutes without the voltage controlled gate. While the purpose of this brief run was to determine the overall data rate, the data set can also be used to find the initial rate of locatable sources and plot those sources. The data set was filtered to remove all sources which appeared to occur at times other than at the peak load. Figure 3 shows the location of these sources and the sum of the number of located sources as a function of time. It is quite apparent from this data that damage in the 18,19,21,20 rectangle started at the first cycle which reached full load. The other oil can region, which occurred in the rectangle 12,13,15,14 showed no sign of locatable emission during this short run. No located emissions were seen in the root area covered by sensors 1 through 9.

The steady occurrence of locatable emission at the peak load of almost every cycle as shown in figure 3 strongly indicates that the peak test load of 9535 lbs. exceeded the strength of this blade design in the region of rectangle 18,19,21,20.

Test Results, Stage 2 and 3

In stage 2, the test was started for a prolonged run. The voltage controlled gate was operational and data was taken when the load was above 8500 lbs. An hour and 18 minutes into the test, equipment problems occurred and loading was stopped. The next morning, stage 3 was started and ran for 23 hours. It was stopped because visual indication of damage in the skin was seen in rectangle 18,19,21,20. In addition, loud audible noises were heard on every cycle. There was also a decrease in blade stiffness. The blade was declared to have failed at this time.

Most of the located emissions in this fatigue test occurred in stages 2 and 3. Figure 4 shows the located emissions in these test stages. Again most of the emissions appear to come from the oil can distortions in rectangle 18,19,21,20. Figure 5 shows the sum of the located sources as a function of time. Thirty-two minutes into the stage 2, there was an order of magnitude decrease in the rate of locatable emissions. A similar behavior is seen in stage 3 (the step between 20 and 28 minutes occurred when the loading was temporarily stopped) Notice that the temporary halt in loading did not change the event rate. The event rate did decrease at 78 minutes. A lower rate then continued, with some fluctuations, to 268 minutes. The rate again declined and ceased entirely at 549 minutes. The overall acoustic emission rate from the blade remained constant for the 23 hours of stage 3 but no events occurred where the acoustic burst excited sensors at all four corners of a rectangle within a 350 microsecond window for the last 14 hours of this stage.

Another way to examine the acoustic emission data is to plot hits from each sensor individually. Figure 6 shows totalized plots of the "energy" (actually the signal strength for each emission burst) as a function of time for sensors on top of the spar. Note that there are no significant changes in slope in any of these curves at 78 minutes (4680 seconds), 268 minutes (16,000 seconds) or 549 minutes (33,000 seconds). Thus the rates of located events have no correlation with acoustic emission rates seen at the individual sensors. Also notice that there was an increase in the "energy" rate around 72000 seconds (20 hours) for all sensors except 20. Closer examination showed that except for sensors 20, 21 and 24, there was an increase in the average "energy" per burst after 20 hours. Sensors 20 and 21 are located near the region where maximum damage occurred. There was very little sound material left in the skin in rectangle 18,19,21,20 by this point in the test. It is probable that this region weakened, transferring more load to the surrounding regions. This should increase the damage and lead to more acoustic energy being produced in each burst. Sensor 24 is a different case. Here the separation from sensor 22 (60 inches) is far enough so that the attenuation would allow few, if any, signals to excite both sensors. The increase here was much larger, proportionally, than that seen in other sensors. The sensor was positioned to try to detect any damage occurring near the loading point on the blade and such damage is probably what is being seen. The average "energy" per burst decreased for sensor 24 beyond the 20 hour point which reinforces the assumption that this is a different mechanism from that seen in the other sensors.

Test Results, Stage 4

Stage 4 covered less than an hour of testing time. There were several halts during the test. The test was terminated at 66 minutes when the blade failed. A halt at 53 minutes was taken just after the skin ripped and separated from the top of the front spar. The test was restarted at 64 minutes and lasted about two minutes when the top skin buckled and ripped from the front spar toward the rear spar. Sensor 20 was just about over the rip and the failure broke the silicone rubber bond and launched sensor 20 skyward.

Figure 7 shows the map of located events for this stage and the located events as a function of time. There were not a large number of events located during this stage. The reason is not the lack of emission, but rather the gross damage in the skin which increased the acoustic attenuation, and the separation of the skin from the spar which interrupted the acoustic path to the rear sensors. These mechanisms prevented the acoustic bursts generated by even very energetic events from triggering all four sensors in a rectangle.

Discussion

There was no indication of any damage occurring in the root region of the blade. The few located emissions were mapped at random over the surface. The totals of the signal strengths from sensors 2 through 9 were orders of magnitude less than those of sensors 18 through 21. There was also no indication of acoustic signals being introduced into the blade from the mounting block.

The location data from all four stages was combined. Figure 8 shows this data plotted in the critical rectangle 18,19,23,22. The symbols on the plot indicate the number of located events per square inch. The highest density is right in the middle of the region showing oil can deformation. Visual observation of this area before the stage 4 run indicated extensive damage. The final failure of the blade also occurred very close to the area of maximum density of located events.

One should note that the highest density of located events is not along the line between sensor 18 and 20 where the initial tear in the skin along the spar took place. The tear effectively prevented any acoustic signals from being transmitted to sensors 19 and

21 and thus prevented location of this failure. For this reason, other types of acoustic emission analysis are often used in composite structures. Figure 6 shows the total signal strength ("energy") as a function of time. Table I shows the total signal strength for several sensors from stage 3.

Table I
Total Signal Strength for Several Sensors in Stage 3
(arbitrary units)

	16) 9.4×10^6
17) 1.4×10^7	
	18) 1.4×10^8
19) 1.1×10^8	
	20) 6.4×10^8
21) 6.7×10^8	
	22) 1.3×10^8
23) 5.5×10^7	

From this table one can see that the center of the damaged area is between sensors 20 and 21 and part way back toward sensors 18 and 19. This corresponds very well with figure 8.

Another way to look for damage is to look at the peak amplitude distributions for different sensors. For a given sensor and material, a higher peak amplitude usually indicates greater damage. (Note that the peak amplitude is measured on a logarithmic scale such that 20 dB corresponds to one order of magnitude). Figure 9 shows the peak amplitude distributions from sensors 13, 17 and 19 for stages 2, 3 and 4. The top graph is stage 2, the middle, stage 3, and the bottom is stage 4. For Stage 1, except for sensor 21, there was essentially no emission with peak amplitudes at or above 80 dB. In stage 3, all sensors but 13 have shown a few hits above 80 dB but they are still in a distinct minority. In stage 4, there are far fewer hits on each sensor but some of the distributions have changed. Sensor 19 now has a distinct peak around 90 dB while 17 is still lacking any signals above 80 dB. This agrees with all of the previous data which indicates failure between sensors 19 and 21. However, we now see peaks with amplitudes above 80 dB for sensor 13. These peaks were not seen in data from sensors 11, 17 nor from sensors 10, 12, 14, and 16. There are few located emissions near the rear spar in this region. The most plausible explanation for this data is that new damage occurred during stage 4 behind the rear spar between sensors 13 and 15. The damaged region would be far enough behind the spar that the attenuation prevents the detection of the signals at sensors 12 and 14.

Conclusions

The acoustic emission data shows that the increase of the load to 9535 lbs. exceeded the static strength of the blade. The skin in the rectangle formed by sensors 18,19,21,20 went into oil can deformation. This oil can deformation was accompanied by degradation of the fiberglass skin. The damage appeared to start as soon as full load was reached. Oil can deformation is not, of itself, detrimental to fiberglass. The skin in the rectangle formed by sensors 12,13,15,14 also showed oil can deformation throughout this test but showed no sign of fiberglass degradation. In stage 4 when the blade was failing, there was indications of another region of failure toward the trailing edge of the blade between sensors 13 and 15.

Acknowledgement

The author would like to thank Jim Johnson, Mike Jenks and all the personnel of the NREL wind turbine testing facility for their valuable help and consultation. He would also like to thank Herb Sutherland of Sandia and Walt Musial of NREL for a critical review of this Paper.

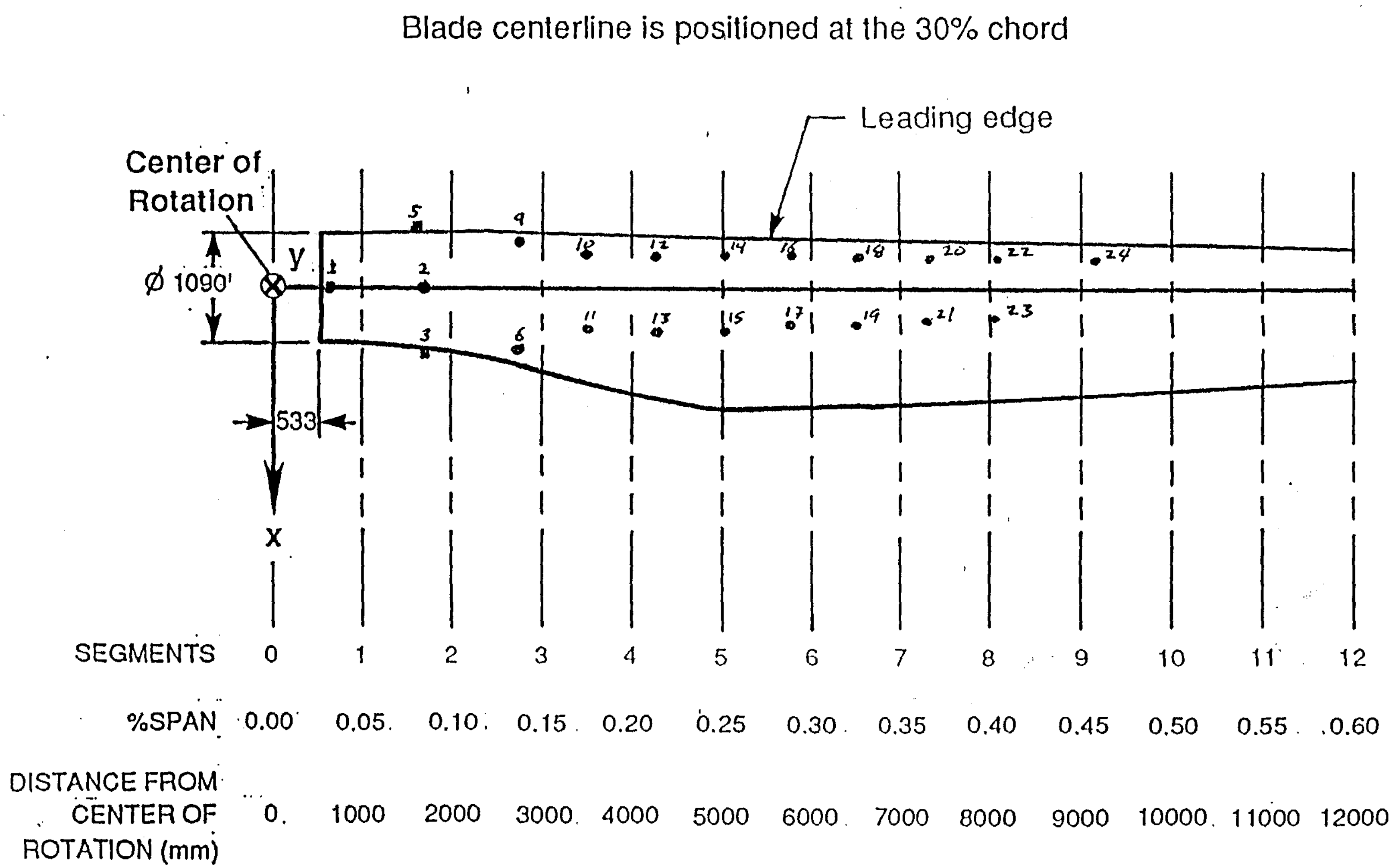

Figure 1. Blade and Sensor Layout

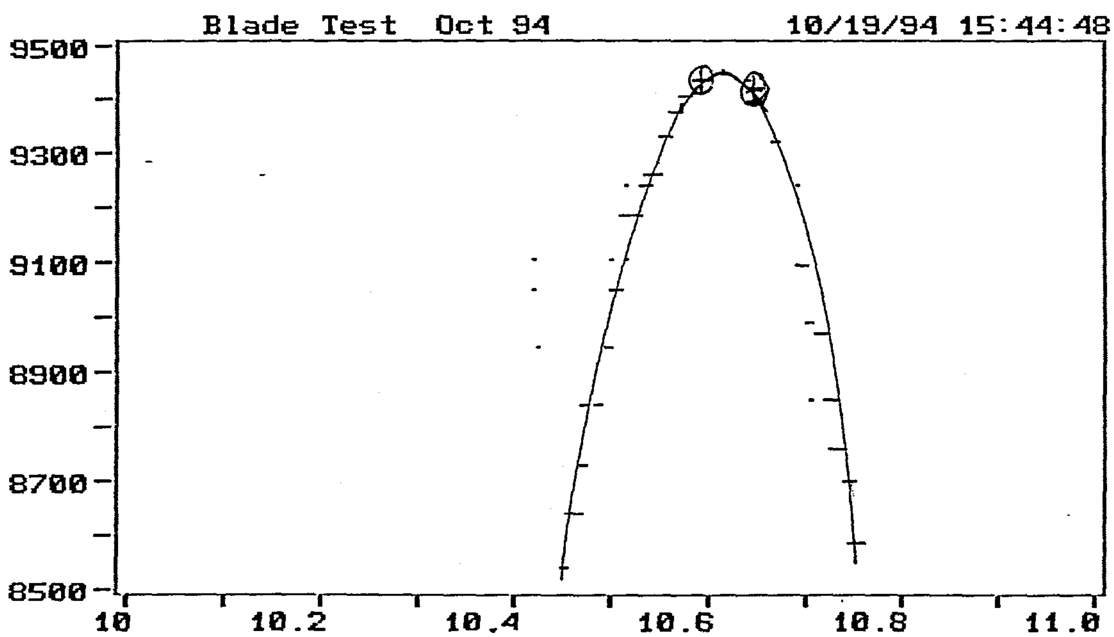

Load (lbs) vs Time (sec)

Figure 2. Load values as a function of time for the peak of a load cycle. Horizontal lines are multiple points.

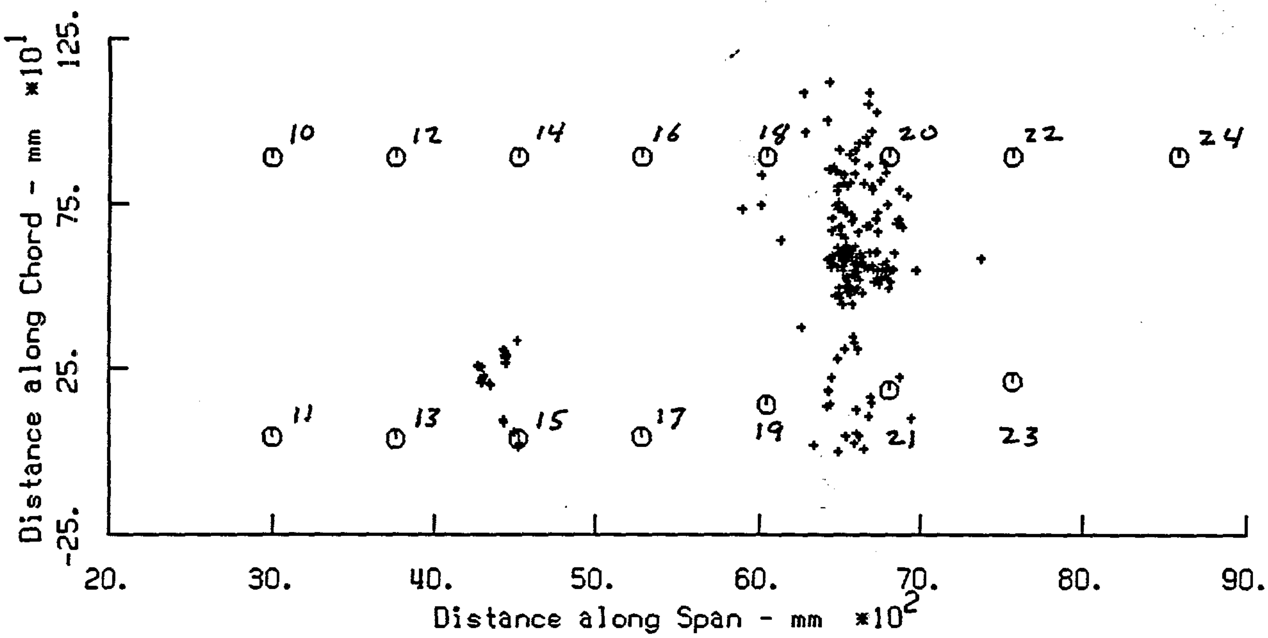

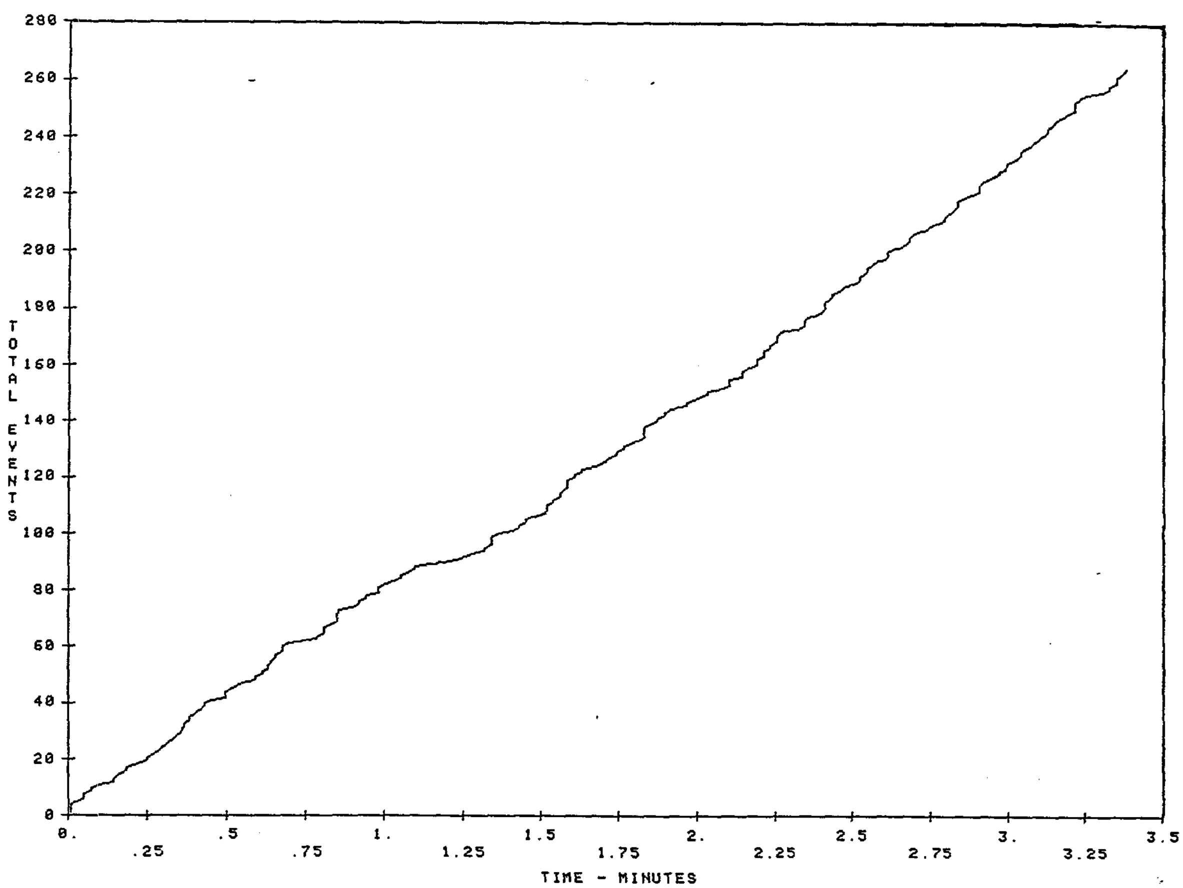

Figure 3. Event Locations and Events as a function of time for Stage 1

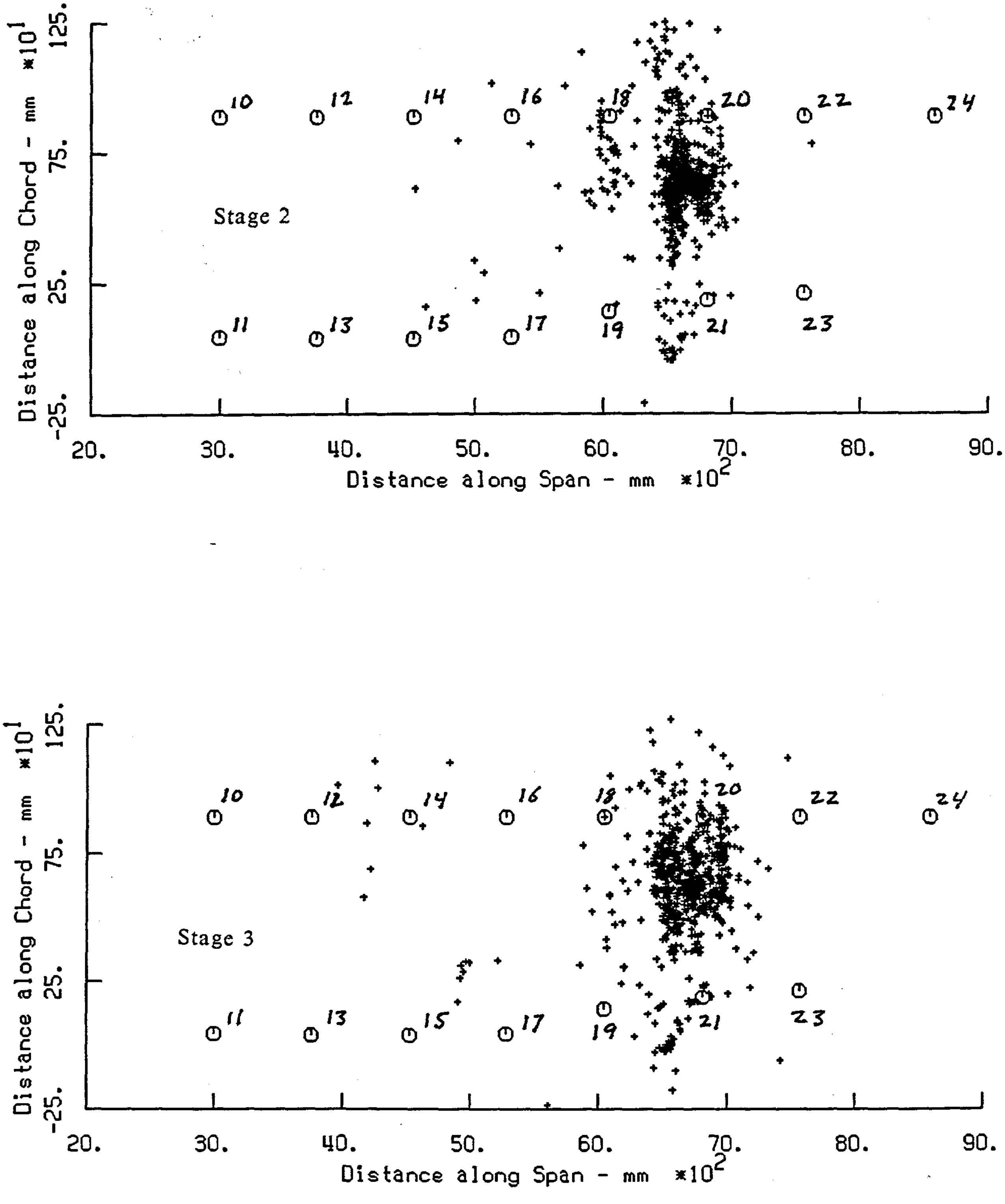

Figure 4. Event Locations for Stage 2 and Stage 3

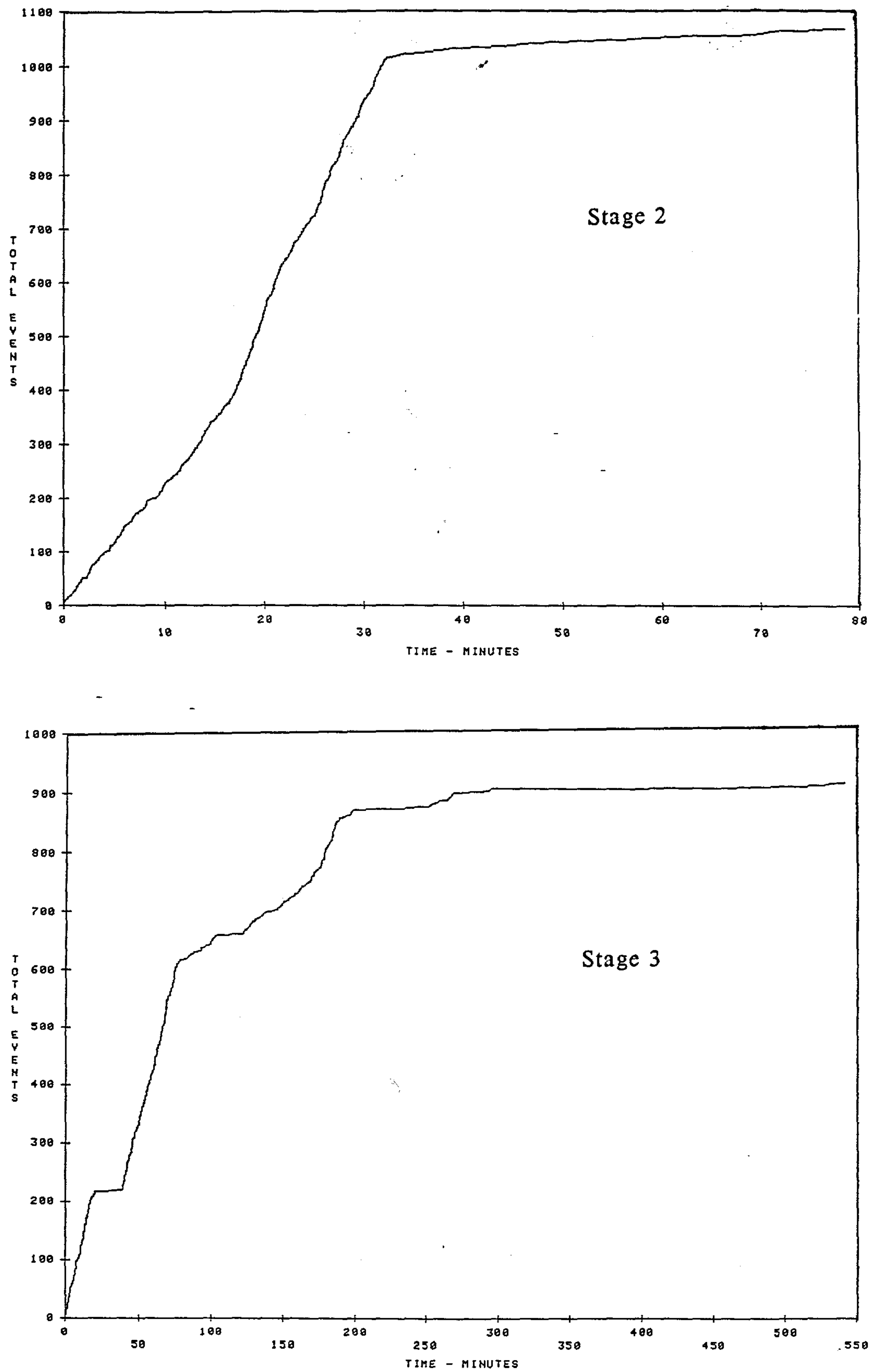

Figure 5. Events as a function of time for Stage 2 and Stage 3

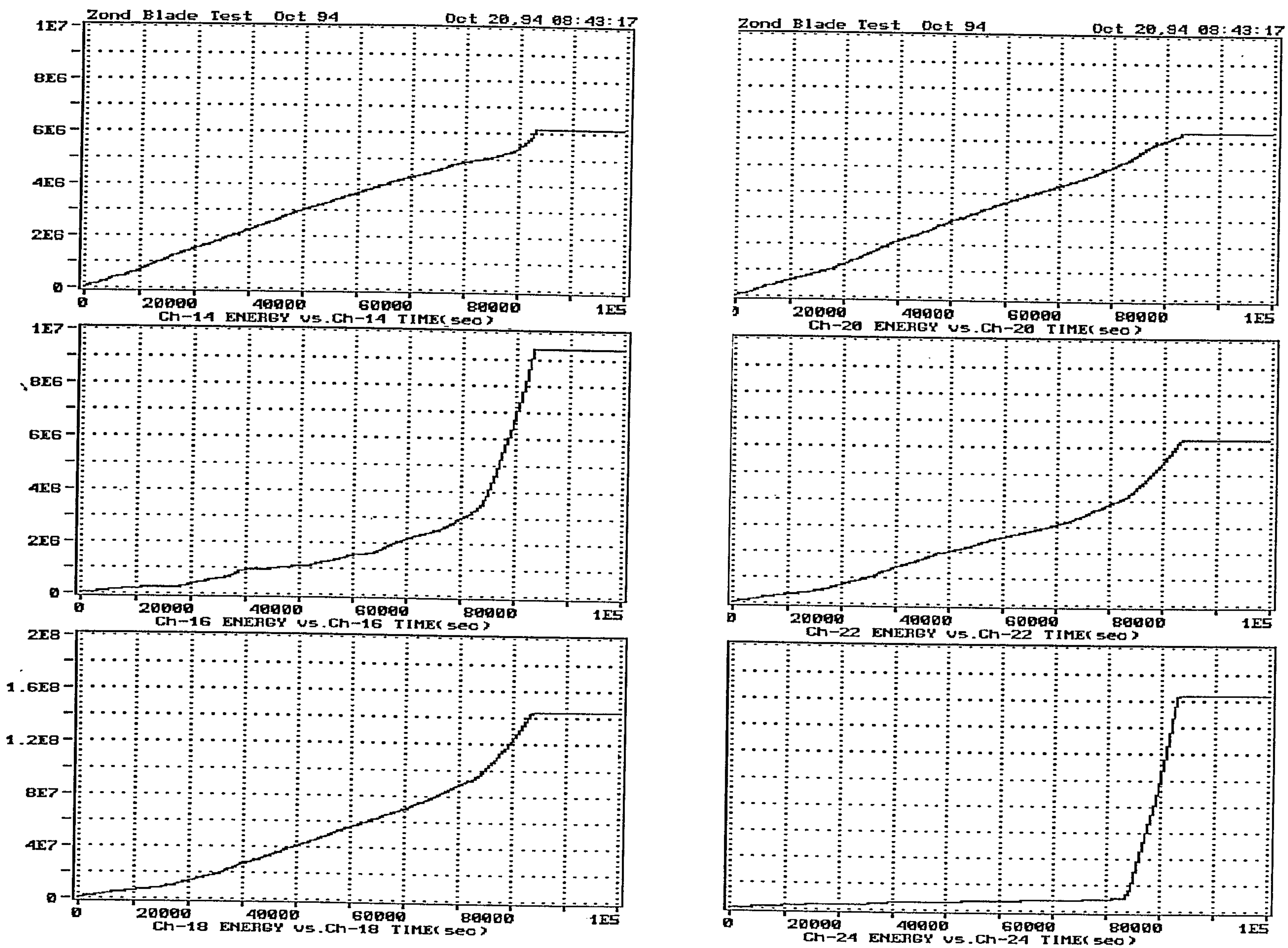

Figure 6. Total "energy" as a function of time for the leading edge sensors.

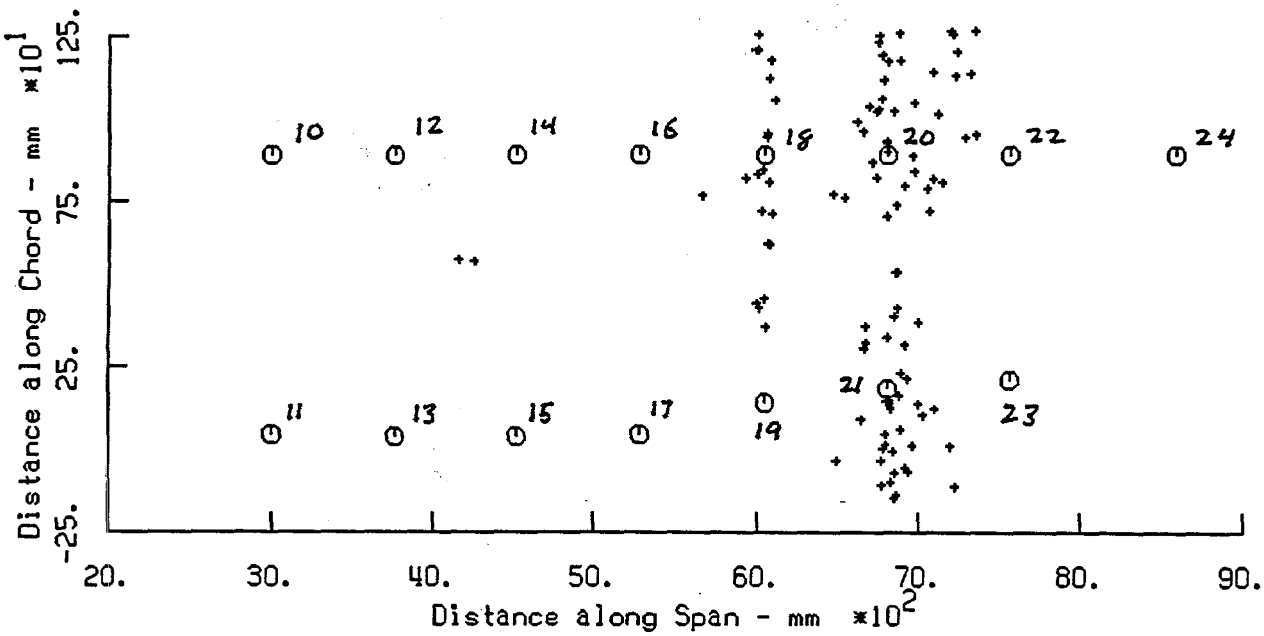

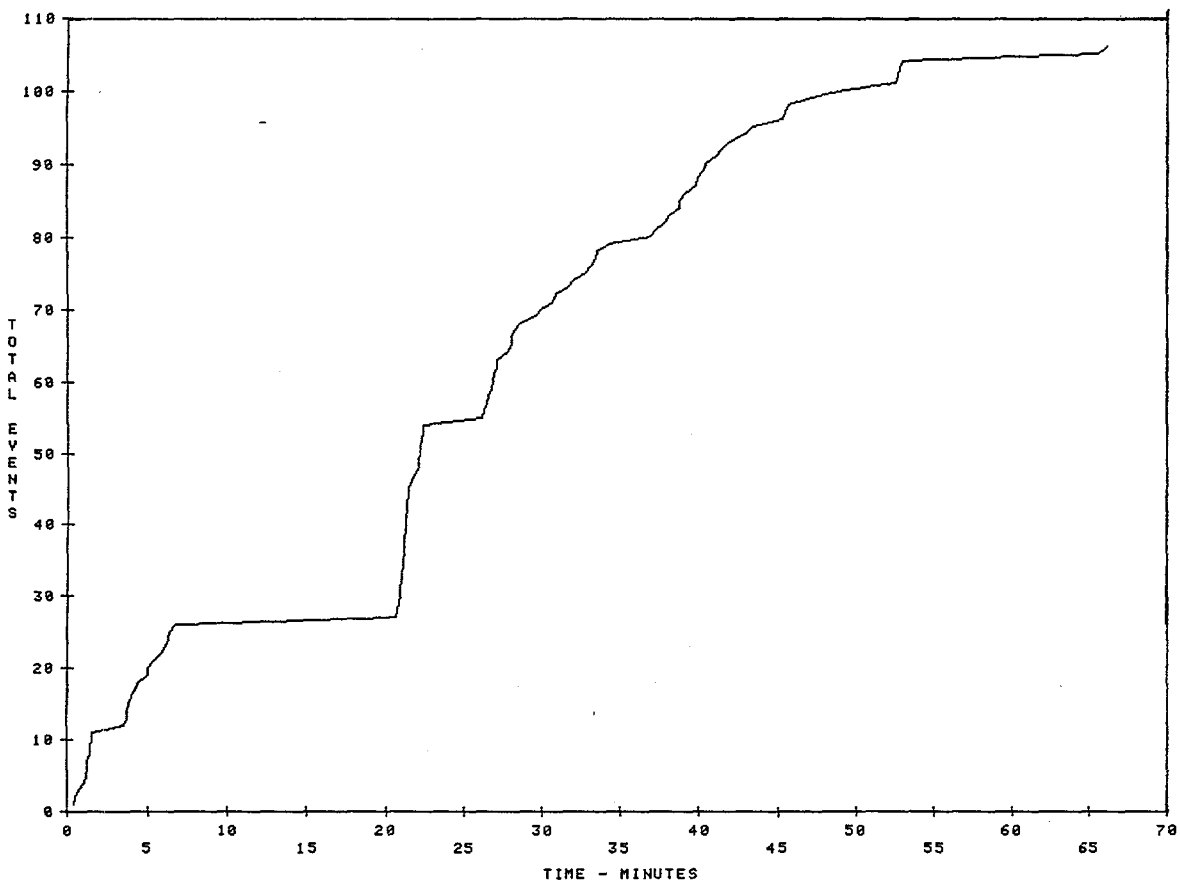

Figure 7. Event Locations and Events as a function of time for Stage 4

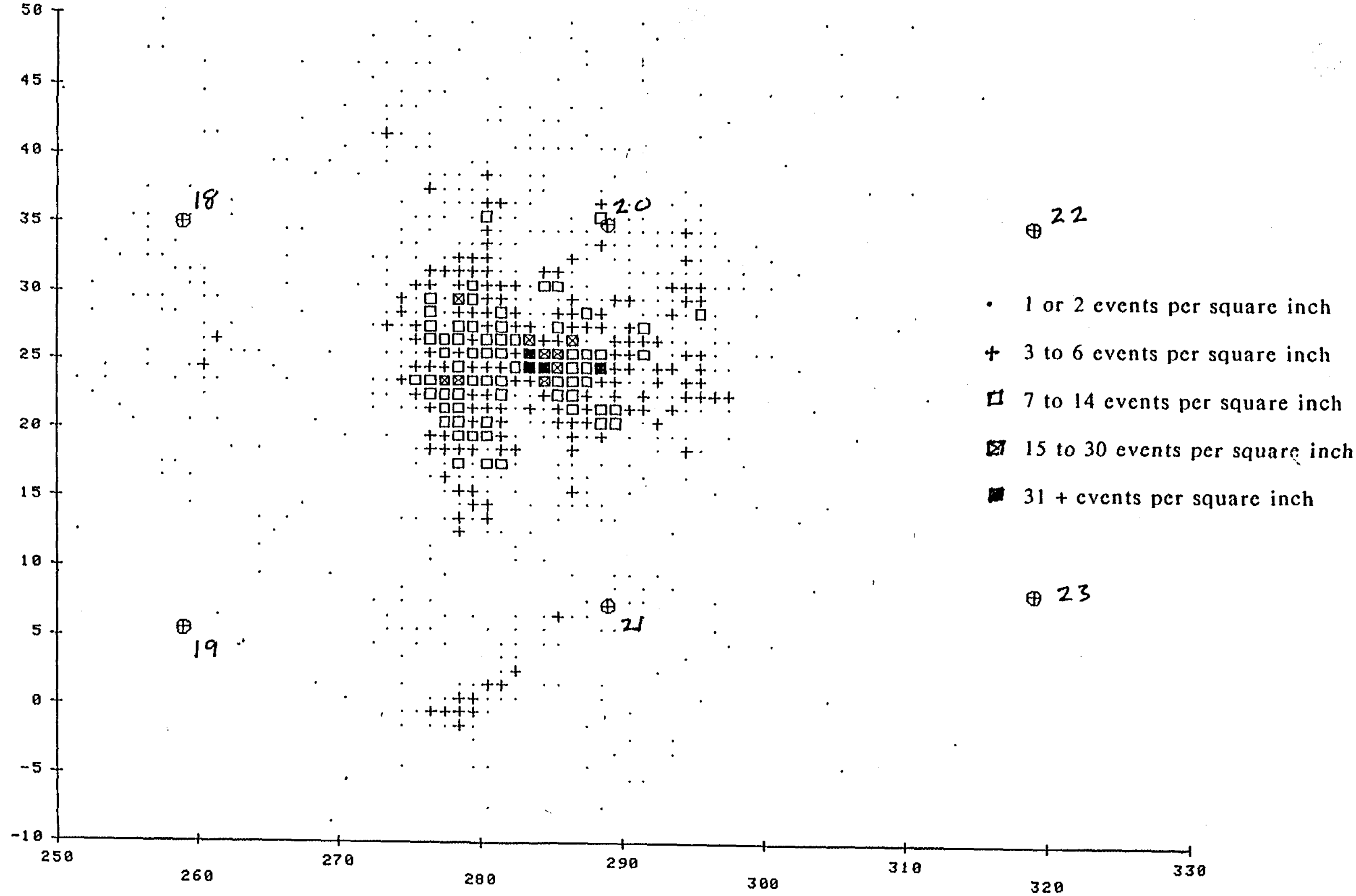

Figure 8. Density of Located Events for the Entire Test.

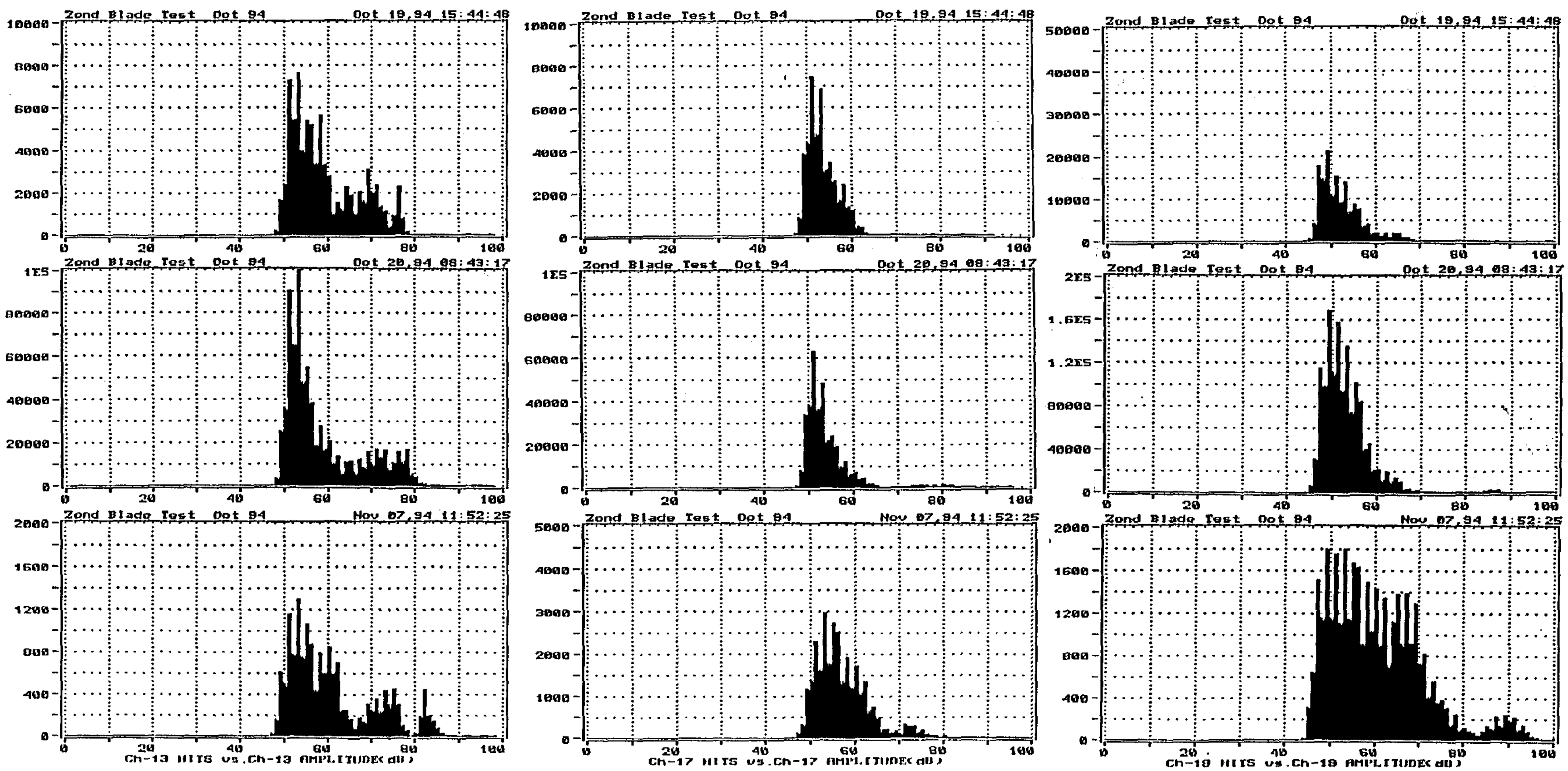

Figure 9. Peak amplitude distributions from Stages 2 (top), 3 (middle) and 4 (bottom) for sensors 13, 17 and 19.